

# Exact determination of the phase structure of the p-species asymmetric exclusion process

M.Khorrami<sup>a,c</sup> 1

V.Karimipour<sup>b,c</sup> 2

<sup>a</sup>*Institue for advanced studies in basic sciences, Gava Zang, P.O.Box 45195-159 , Zanjan, Iran*

<sup>b</sup>*Department of Physics, Sharif University of Technology, P.O.Box 11365-9161, Tehran, Iran*

<sup>c</sup>*Institute for Studies in Theoretical Physics and Mathematics, P.O.Box 19395-5746, Tehran, Iran.*

## Abstract

We consider the p-species generalization of the Asymmetric Simple Exclusion Process (p-ASEP) on an open chain, in which particles hop with their characteristic hopping rates and fast particles can overtake slow ones. We determine exactly the phase structure of this model and show how the phase diagram of the 1-species ASEP is modified. Depending on the distribution of hopping rates, the system can exist in a three-phase regime or a two phase regime. In the three- phase regime the phase structure is almost the same as in the one species case, that is, there are the low density, the high density and the maximal current phases, while in the two-phase regime there is no high density phase.

---

<sup>1</sup>e-mail:mamwad@netware2.ipm.ac.ir

<sup>2</sup>e-mail:vahid@netware2.ipm.ac.ir

# 1 Introduction

The asymmetric simple exclusion process [1, 2, 3, 4, 5, 6] refers to a collection of Brownian particles which under the influence of a driving force, do biased random hopping on a one dimensional lattice and interact via hard core repulsion with each other. In the totally asymmetric case each particle is injected to the system from the left with rate  $\alpha$  and hops only to the right neighboring site with a rate normalized to unity and finally is extracted at the right end with rate  $\beta$ .

This is a model far from equilibrium with many re-interpretations which makes it a suitable model for studying such phenomena as diverse as surface growth [7], and traffic flow [8] [9],(see [10],[6, 11, 12] and references therein.)

One of the most interesting aspects of this process is the possibility of boundary induced phase transitions. It has been observed through various types of solutions [13, 14, 15] that by changing the rate of injection and extraction of particles, different phases will develop in the system. The phase diagram of the model representing the macroscopic current of the particles in various domains in the  $\alpha - \beta$  plane is depicted in fig.(1).

Although many of the characteristics of the process have been obtained [13] [14],[16] before the advent of the Matrix Product Ansatz (MPA) [17], the latter method has proved useful [15] for both obtaining the same results in much simpler ways and in being amenable to further generalizations[18, 19, 20, 21, 22, 23, 24, 25, 26]. In this method the probabilities  $P(\tau_1 \cdots \tau_L)$  , where  $\tau_i$  is the random variable associated with site  $i$  (being 0 for empty site and 1 for an occupied site), is written as:

$$P(\tau_1, \cdots, \tau_L) = \frac{1}{Z_L} \langle W | \prod_{i=1}^L (\tau_i D + (1 - \tau_i) E) | V \rangle \quad (1)$$

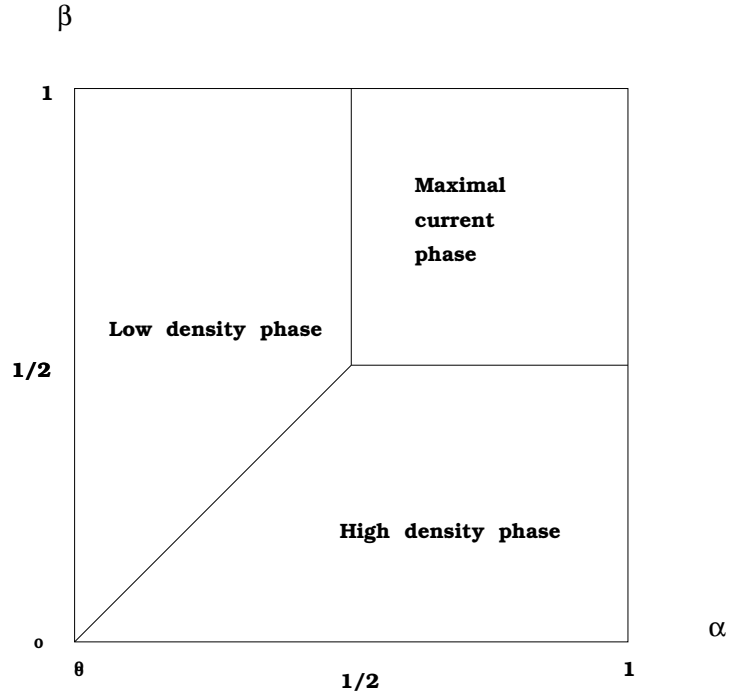


**Figure 1**

Figure 1: Phase diagram of the single species ASEP

where the operators  $D$  and  $E$ , and the vectors  $\langle W |$  and  $|V \rangle$  satisfy the following relations:

$$DE = D + E \quad (2)$$

$$D|V \rangle = \frac{1}{\beta}|V \rangle \quad (3)$$

$$\langle W |E = \frac{1}{\alpha}\langle W | \quad (4)$$

In (1),  $Z_L$  is a normalization constant and is suitably called the partition function. Its value is given by

$$Z_L = \langle W |C^L|V \rangle \quad (5)$$

where  $C := D + E$ .

The question of a natural  $p$ -species generalization of the ASEP, so that in the special case  $p = 1$ , one obtains the results of the one species ASEP [19], has been answered in the affirmative in [20, 21], by postulating a

generalization of the algebra (2-4), which we call the  $p$ -ASEP algebra. The  $p$ -ASEP algebra is generated by  $p + 1$  generators  $E$  and  $D_1 \cdots D_p$  subject to the following relations:

$$D_i E = \frac{1}{v_i} D_i + E \quad (6)$$

$$D_j D_i = \frac{1}{v_i - v_j} (v_i D_j - v_j D_i) \quad j > i \quad (7)$$

$$D_i |V\rangle = \frac{v_i}{v_i + \beta - 1} |V\rangle \quad (8)$$

$$\langle W | E = \frac{1}{\alpha} \langle W | \quad (9)$$

In this algebra the parameters  $v_i$  are real positive numbers which are ordered as  $v_1 \leq v_2 \cdots \leq v_p$ .

The process described by this algebra is one in which each particle of type  $i$  arrives at the left end with rate

$\alpha_i := \frac{1}{p} \alpha v_i$ , hops to its right neighboring empty site with rate  $v_i$  and leaves the system at the right end with

rate  $\beta_i = \beta + v_i - 1$ . If this particle encounters on its way a site occupied by a particle of type  $j$  with  $j < i$ ,

it will overtake it with rate  $v_i - v_j$ , otherwise it stops. For all the extraction rates  $\beta_i$  to be positive we also

require that  $\beta \geq 1 - v_1$ . The unit of time is set so that the average hopping rate is unity, i.e:  $\frac{1}{p} \sum_{i=1}^p v_i = 1$ .

Thus the parameters  $\alpha$  and  $\beta$  are respectively the total injection rate and the average extraction rate of the particles respectively. Note that all the elementary processes are stochastic, i.e: in a time interval  $dt$ , a particle of type  $i$  present in a given site, hops to the right empty site with probability  $v_i dt$ , and does not move with probability  $1 - v_i dt$ .

The model we consider depends on two boundary parameters  $\alpha$  and  $\beta$  and a set of intrinsic hopping rates  $v_1, \dots, v_p$ . More appropriately the information on the hopping rates is encoded in a distribution function  $\sigma(v)$ , where  $\sigma(v)dv$  is the probability that a particle has a hopping rate between  $v$  and  $v + dv$ . Here we have assumed for definiteness that the random hopping rates are taken from a continuous distribution. All our arguments below are however valid also for a discrete distribution, for which  $\sigma(v) := \frac{1}{p} \sum_i \delta(v - v_i)$ .

The main motivation for pursuing this problem is to see how the phase structure of the one-species ASEP (hereafter denoted by 1-ASEP) is modified, when we have particles with a variety of hopping rates and specially when particles can overtake each other. Do we still have the phases of low-density, high-density and maximum current, present in the 1-ASEP, or it is changed in an essential way?. How the variety of hopping rates in the bulk or their probability distribution enter the picture and what role they play in the phase structure of the system ? How the absence of pharticle-hole symmetry in this model is reflected in the phase diagram?

We will go through these questions by providing an exact solution of this problem, and will obtain a generalization of the phase diagram of the 1-ASEP.

As far as we consider only the mean field line  $\alpha + \beta = 1$  [20], one dimensional representations of the algebra (6-9) give an exact solution. However to uncover the important role of fluctuations, we should explore the full  $\alpha - \beta$  plane and for this we should use the infinite dimensional representation. What we will do is to calculate exactly the generating function for partition functions of systems with different sizes and by carrying out an analysis of its singularities, determine the currents and the different phases of the system. The phase structure depends on the values of  $\alpha$ ,  $\beta$ , and on the characteristics of the distribution function.

## Main Results:

- To every distribution function  $\sigma(v)$  of hopping rates, we can assign a real number  $l[\sigma]$ , which essentially depends on the behaviour of  $\sigma(v)$  for small hopping rates (i.e: if  $\sigma(v) = 0$  or not and if yes how slowly it approaches this value). The parameter  $l_c = 0$  is special in the sense that for all distribution functions with  $l[\sigma] < 0$ , the phase diagram of the  $p$ -ASEP is almost the same as the phase diagram of 1-ASEP, that is, in the  $\alpha - \beta$  plane we have three regions of low density, high density and maximum current phases. The value

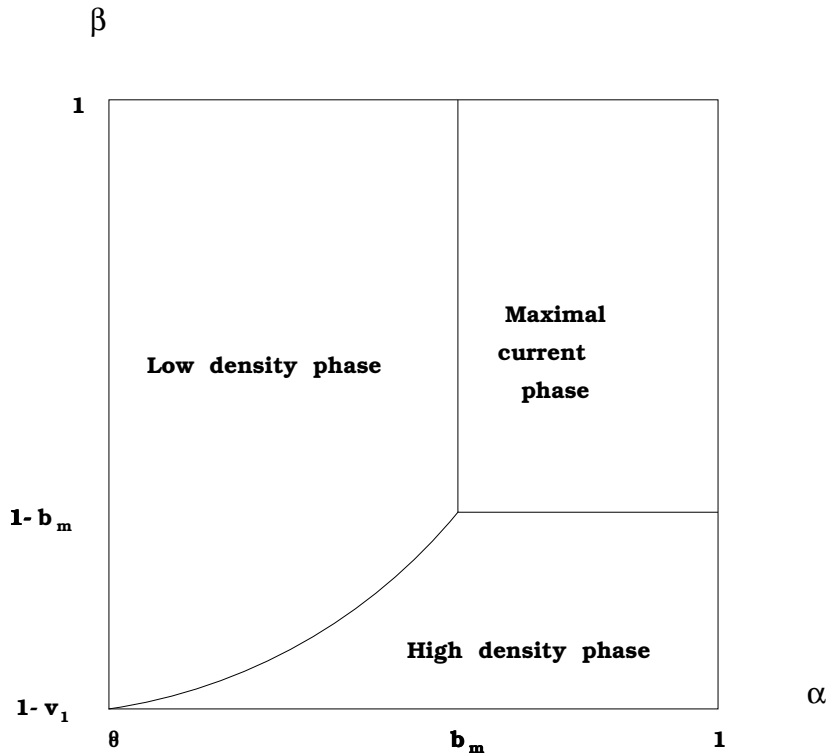


Figure 2: Phase diagram of multi-species ASEP when  $l[\sigma] < 0$

of the maximum current and the shape of the coexistence curves between different phases depend on the distribution function (see figs.(2)and (3)). We also obtain the average density of all types of particles in all three phases.

- If on the other hand  $l[\sigma] \geq 0$ , then the phase diagram consists of only two phases, namely the low density and the maximum current phase. The extraction rate  $\beta$  does not have any effect on the system and only the injection rate  $\alpha$  determines which phase will develop in the system (fig.4). We also obtain the average density of all types of particles in both phases.

Thus the general shape of the phase diagram is controlled by three parameters. The two control pa-

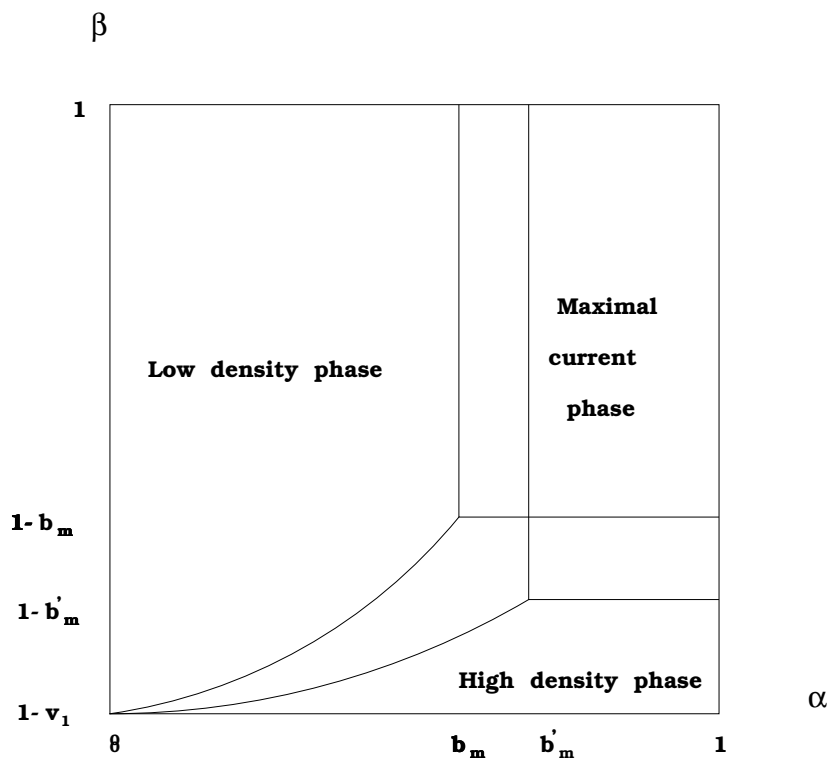


Figure 3: Phase diagram of the multi-species ASEP for two different probability distributions of hopping rates, superimposed on each other

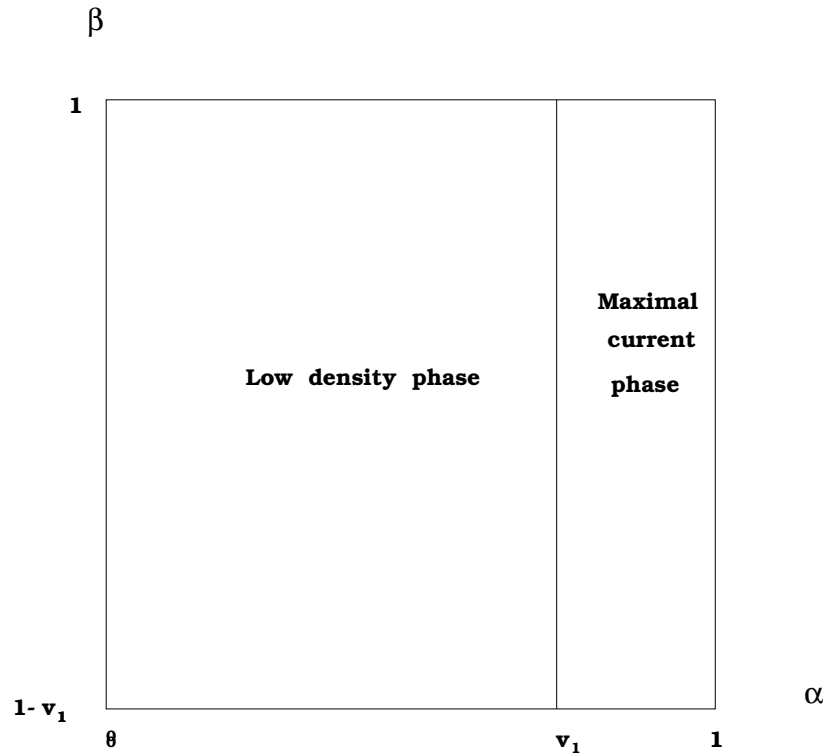


Figure 4: Phase diagram of the multi-species ASEP when  $l[\sigma] > 0$

parameters  $\alpha$  and  $\beta$  represent the effect of boundaries and the third parameter  $l[\sigma]$ , takes into account the distribution function of hopping rates.

This paper is organized as follows: In section (2), we introduce the necessary preliminary material from [20] and set our notations and conventions. In section (3) the generating functions for the currents and average density of particles of each species are introduced and the former one is calculated exactly. In section (4) the total current is calculated in terms of which the different phases of the system are determined. Section (5) is devoted to the calculation of the generating function for the average densities and the calculation of latter quantities. In section (6) we discuss two special cases, namely the 1-ASEP where we reproduce the already known results, and the case when one of the hopping rates is much smaller than the others. We conclude the paper with a discussion in section (6).

## 2 Some algebraic preliminaries

To make the present paper self-contained, we quote the basic definitions and theorems from [20], to which the reader can refer to, for further details and proofs.

The algebra (6-9) has only one or infinite dimensional representations. We write the infinite dimensional representation in a convenient basis consisting of vectors  $|0>, |1>, \dots |p>$ , with the following actions:

$$E|n> = |n+1> \quad (10)$$

$$D_i|n> = v_i^{-n}d_i|0> + v_i^{-n+1}|1> + v_i^{-n+2}|2> + \dots v_i^{-1}|n-1> + |n> \quad (11)$$

We also have:

$$|V> = \sum_{n=0}^{\infty} (1-\beta)^n |n> \quad (12)$$

$$<W| = \sum_{n=0}^{\infty} (\alpha)^{-n} < n| \quad (13)$$

The basis  $\{< n|\}$  is the dual of the basis  $\{|n>\}$ , i.e:  $< n|m> = \delta_{n,m}$ .

The operator  $C$  is defined as

$$C := E + \frac{1}{p}(D_1 + D_2 + \dots + D_p) \quad (14)$$

whose action on the basis vectors is calculated to be

$$C|n> = \sum_{k=0}^{n+1} < \frac{1}{v^{n-k}} |k> \quad (15)$$

where  $< \frac{1}{v^k} >$  is the average of the inverse  $k$ -th power of the hopping rates. ( $< \frac{1}{v^k} > = \frac{1}{p} \sum_{j=1}^p \frac{1}{(v_j)^k}$  for discrete distributions and  $< \frac{1}{v^k} > = \int dv \sigma(v) \frac{1}{v^k}$  for continuous distributions). The explicit matrix form of  $C$

is :

$$C = \begin{pmatrix} 1 & <\frac{1}{v}> & <\frac{1}{v^2}> & <\frac{1}{v^3}> & <\frac{1}{v^4}> & \dots \\ 1 & 1 & <\frac{1}{v}> & <\frac{1}{v^2}> & <\frac{1}{v^3}> & \dots \\ 0 & 1 & 1 & <\frac{1}{v}> & <\frac{1}{v^2}> & \dots \\ 0 & 0 & 1 & 1 & <\frac{1}{v}> & \dots \\ 0 & 0 & 0 & 1 & 1 & \dots \\ \vdots & \vdots & \vdots & \vdots & \vdots & \ddots \\ \vdots & \vdots & \vdots & \vdots & \vdots & \ddots \\ \vdots & \vdots & \vdots & \vdots & \vdots & \ddots \end{pmatrix}. \quad (16)$$

Clearly direct evaluation of the  $N$ -the power of this matrix is a formidable task. In the one species case

where  $\frac{<1>}{v^k} = 1, \forall k$ , one can go to a new basis  $\{|n>':= (E - 1)^n |0>\}$  in which the matrix  $C$  becomes tri-diagonal with the simple form  $C_{n,m} = 2\delta_{n,m} + \delta_{n,m+1} + \delta_{n,m-1}$ . This Hermitian matrix can then be either easily diagonalized [15] or else, yield simple recursion relations which can be solved by an analogy with the master equation of a random walk in the presence of an absorbing wall [15]. Due to the complicated form of the matrix  $C$ , none of the above strategies work in the present case. The same is true with the method of repeated application of the algebraic relations (6-9) and calculating directly the matrix element  $\langle W|C^N|V \rangle$  [15].

There is however one basis in which a managable recursion relation can be found, namely the coherent basis defined as follows:

$$|u> = \sum_{n=0}^{\infty} u^n |n> \quad (17)$$

$$\langle u| = \sum_{n=0}^{\infty} u^n \langle n|. \quad (18)$$

Note a slight difference of our notation with that of [20] in the symbol for  $\langle u |$ , where this state would have been denoted by  $\langle u^{-1} |$ . These states have the following properties:

$$\langle u | E = u \langle u | \quad (19)$$

$$D_i |u\rangle = \frac{v_i}{v_i - u} |u\rangle \quad (20)$$

$$\langle \omega | u \rangle = \frac{1}{1 - u\omega} \quad \text{for} \quad |u\omega| < 1 \quad (21)$$

$$\oint_c \frac{du}{2\pi i u} |u\rangle \langle u^{-1}| = 1 \quad (22)$$

where  $c$  is any contour encircling the origin.

**Remark:** In calculation of matrix elements of operators between two states  $\langle a |$  and  $|b \rangle$ , one can insert any numbers of unit operators in the form of (22) with integration variables  $u_1, u_2, \dots$  from left to right, provided that  $|\frac{1}{a}| > |u_1| > |u_2| > \dots > |b|$ . This is due to the restriction (21). The results of such calculations are then valid only for  $|ab| < 1$  and must be analytically continued to larger domains. From the definition of  $C$  and (19)-(21) one obtains

$$\langle u | C | w \rangle := \left( u + \frac{1}{p} \sum_i^p \frac{1}{1 - w/v_i} \right) \left( \frac{1}{1 - uw} \right) \quad (23)$$

for discrete distributions and

$$\langle u | C | w \rangle := \left( u + \int dv \sigma(v) \frac{1}{1 - w/v} \right) \left( \frac{1}{1 - uw} \right) =: \left( u + g(w) \right) \left( \frac{1}{1 - uw} \right) \quad (24)$$

where the second equality defines the function  $g(w)$ , a shorthand and useful notation for which is

$$g(w) = \left\langle \frac{1}{1 - w/v} \right\rangle. \quad (25)$$

Here the average is taken with respect to the probability distribution of hopping rates,  $\sigma(v)$ .

### 3 The generating functions for current and average densities

The total current for a system consisting of  $N$  sites has been found to be [20]

$$J = \frac{\langle a|C^{N-1}|b \rangle}{\langle a|C^N|b \rangle}, \quad (26)$$

Where  $\langle a|$  and  $|b \rangle$  are coherent states and for convenience, we have denoted  $1 - \beta$  by  $b$ , and  $\alpha^{-1}$  by  $a$ .

The current of each species, say the  $i$ -th one is given by

$$J_i = \frac{v_i}{p} J \quad (27)$$

In the thermodynamic limit  $N \rightarrow \infty$ , there is a simple way to obtain this expression. Define a generating function

$$f(s; a, b) := \sum_{N=0}^{\infty} s^N \langle a|C^N|b \rangle \quad (28)$$

The convergence radius of this formal series,  $R$ , is precisely what we need. In fact

$$R = \lim_{N \rightarrow \infty} \frac{\langle a|C^{N-1}|b \rangle}{\langle a|C^N|b \rangle}. \quad (29)$$

**Remark:** The function  $f(s; a, b)$  has a taylor-series expansion in terms of (non-negative) powers of its three arguments, which means that there is a region containing the origin of the space  $C^3$ , where  $f$  is analytic. This is easily seen from the algebraic relations (6).

The radius of convergence is also the absolute value of the nearest singularity of  $f$  to the origin. We also know that all of the coefficients of the taylor expansion of  $f$  in terms of  $s$  are positive. This assures that the nearest singularity of  $f$  lies in fact on positive real half-line. That is, the current at the thermodynamic limit is real and positive, as it should be. A similar method works for the average density of particles of each species as well. The global density of particles of type  $i$  is

$$\rho_i = \frac{1}{N} \sum_{k=1}^N \frac{\langle a|C^{k-1} \frac{D_i}{p} C^{N-k}|b \rangle}{\langle a|C^N|b \rangle}. \quad (30)$$

To obtain this, we use fugacities  $z_i$  to define an operator  $C(\mathbf{z})$  as

$$C(\mathbf{z}) := z_0 E + \sum_{i=1}^p z_i \frac{D_i}{p}. \quad (31)$$

Note that we have  $C(\mathbf{1}) = C$ , where by  $\mathbf{1}$  we mean a vector all of whose entries are 1. It is straightforward to see that

$$\rho_i = \frac{z_i}{N} \frac{\partial}{\partial z_i} \ln \langle a | C^N(\mathbf{z}) | b \rangle \Big|_{\mathbf{z}=\mathbf{1}}. \quad (32)$$

Once again, the right-hand of this can be expressed in terms of the radius of convergence  $R(\mathbf{z})$  of a formal series  $f(\mathbf{z}; s, a, b)$  defined as:

$$f(\mathbf{z}; s; a, b) := \sum_{N=0}^{\infty} s^N \langle a | C^N(\mathbf{z}) | b \rangle. \quad (33)$$

Using an equivalent definition for the radius of convergence as  $R(\mathbf{z}) := \lim_{N \rightarrow \infty} \left( \langle a | C^N(\mathbf{z}) | b \rangle \right)^{\frac{-1}{N}}$ , we

have:

$$\rho_i = z_i \frac{\partial}{\partial z_i} \ln \frac{1}{R(\mathbf{z})} \Big|_{\mathbf{z}=\mathbf{1}}. \quad (34)$$

So the key step in obtaining the physical quantities is to calculate the functions (28) and (33), which we call the generating functions for currents and average densities respectively.

### 3.1 Exact calculation of the generating function $f(s; a, b)$

First we use (24) to obtain a recursion relation for  $\langle a | C^N | b \rangle$ :

$$\begin{aligned} \langle a | C^{N+1} | b \rangle &= \oint \frac{du}{2\pi i u} \langle a | C^N | u \rangle \langle u | C | b \rangle \\ &= \oint \frac{du}{2\pi i u} \langle a | C^N | u \rangle \left[ g(b) + \frac{1}{u} \right] \frac{1}{1 - b/u}. \end{aligned} \quad (35)$$

Multiplying both sides of (35) by  $s^N$  and summing over  $N$  from zero to infinity, we arrive at

$$\frac{1}{s} [f(s; a, b) - f(0; a, b)] = \oint \frac{du}{2\pi i u} f(s; a, u) \left[ g(b) + \frac{1}{u} \right] \frac{1}{1 - b/u}. \quad (36)$$

The generating function which we calculate in this way will be restricted to the domain  $|ab| < 1$ . After calculating it for this region of parameters, we will analytically continue it for other values of parameters as well. Since  $|\frac{1}{a}| > |u| > |b|$  the integrand in the right-hand side of (36) has just two poles inside the integration contour; one at  $u = 0$  and the other at  $u = b$ . This is true provided  $f(s; a, u)$  itself is analytic for  $u$  inside the integration contour. However, we know that for small values of its arguments the function  $f(s; a, u)$  is analytic (see the remark after eq. (29)). The result of this calculation will be valid for small values of the arguments of the generating function. One can then use analytic continuation to obtain more general results. Knowing the nonanalytic structure of the integrand, one can use Cauchy's theorem to evaluate the right-hand side of (36):

$$\frac{1}{s}[f(s; a, b) - f(0; a, b)] = -\frac{f(s; a, 0)}{b} + \left[ \frac{1}{b} + g(b) \right] f(s; a, b). \quad (37)$$

Solution of this equation for  $f(s; a, b)$  yeilds

$$f(s; a, b) = \frac{sf(s; a, 0) - b f(0; a, b)}{b\{s[g(b) + 1/b] - 1\}} \quad (38)$$

Note that from (28)

$$f(0; a, b) = \langle a | b \rangle = \frac{1}{1 - ab}, \quad (39)$$

and  $g(b) \equiv \left\langle \frac{1}{1 - \frac{b}{v}} \right\rangle$  is a function which can be determined once the data of the problem (i.e: the distribution function  $\sigma(v)$  ) are given. Equation (38) then suggests that  $f(s; a, b)$  is known, provided a two-variable restriction of it, namely  $f(s; a, 0)$  is known. Eq.(38) contains even more information. To see this, notice that from (38) it seems that there is a pole for  $s$  at

$$s_0 = S(b) := \frac{1}{g(b) + 1/b} \quad (40)$$

From the definition of  $g(b)$ , it is seen that, as  $b$  tends to zero,  $g(b)$  tends to unity. So, for small values of  $b$ ,  $S(b)$  behaves like  $b$ :

$$S(b) \sim b + O(b^2), \quad \text{as } b \rightarrow 0. \quad (41)$$

But this means that as  $b$  tends zero, the radius of convergence for the variable  $s$  tends to zero, and this can not be the case, due to the remark after (28). To avoid this apparent paradox, it must be true that  $s = S(b)$  must not really be a pole, at least for small values of  $b$ . This means that the numerator in (38) must also vanish for  $s = S(b)$ . For this to be the case, we should have

$$S(b) f[S(b); a, 0] = b f(0; a, b) = \frac{b}{1 - ab}. \quad (42)$$

This equation allows us to determine the function  $f(s; a, 0)$  and hence via (38), the complete generating function. Denoting the inverse function of  $S$  by  $B$ :

$$S[B(s)] = s, \quad (43)$$

we find

$$f(s; a, 0) = \frac{1}{s} \frac{B(s)}{1 - aB(s)}. \quad (44)$$

Note, however, that  $S$  is not in general one to one and in different domains of its arguments it has different inverses. In fact we will show later that  $S$  is at most a two-to-one function with the property  $S(0) = 0$ . By the inverse  $B$  we mean the one that tends to zero as its argument tends to zero:

$$\lim_{s \rightarrow 0} B(s) = 0. \quad (45)$$

Inserting (44) in (38), and using (42), we find

$$f(s; a, b) = \frac{\frac{B(s)}{1 - aB(s)} - \frac{b}{1 - ab}}{b \left[ \frac{s}{S(b)} - 1 \right]}. \quad (46)$$

This is the final form of the generating function. For any given probability distribution of hopping rates, one can obtain  $S(b)$  and hence  $B(s)$  from (25), and (40), which after insertion into (46) gives the complete generating function. What we will do in the next sections is to carry out an analysis of the singularity structure of this function and determine the currents and hence the different phases of our multi-species stochastic process. Our results and analysis depend on the general behaviour of the functions  $S(b)$  and  $B(s)$  which in turn depend on the distribution of hopping rates.

## 4 The total current and the phase structure of the system

As it was seen in the previous section, to investigate the properties of the system, one must know the behaviour of the function  $S$ . We have

$$\frac{1}{S(b)} = \frac{1}{b} + g(b). \quad (47)$$

The function  $1/b$  is decreasing (for  $b > 0$ ), while  $g(b)$  is increasing (for  $0 < b < v_1$ ). We remind that  $v_1$  is the smallest hopping rate of the particles.

The function  $S(b)$  has the following properties as can be verified directly from its definition (47):

**1-** $S(0) = 0$  and  $S'(0) = 1$ .

**2-** It is convex in its domain of definition, since

$$\frac{d^2}{db^2} S^{-1}(b) = \frac{2}{b^3} + \left\langle \frac{2v}{(v-b)^3} \right\rangle > 0.$$

**3-**It has a simple singularity at  $b = v_1$  for discrete distributions of hopping rates. For continuous distribution,  $S(b)$ , as a function of the *complex* variable  $b$ , has a branch cut on a segment of the real line beginning from

$b = v_1$ . To see this we use  $\frac{1}{x \pm i\epsilon} = pf(\frac{1}{x}) \mp i\pi\delta(x)$  to obtain

$$\frac{1}{S(b + i\epsilon)} - \frac{1}{S(b - i\epsilon)} = 2\pi i b \delta(b).$$

The phase structure depends crucially on whether  $S$  attains a local maximum in this domain or not. This is easily checked by calculating  $\frac{d}{db}S(b)\Big|_{b=v_1}$ . That is whether the parameter

$$l := \frac{1}{v_1^2} - \left\langle \frac{v}{(v - v_1)^2} \right\rangle \quad (48)$$

is greater or less than zero. This last property is determined *only by the probability distribution of hopping rates* and this is where this function plays its essential role. To emphasise the dependence on the distribution function we denote the quantity in (48) by  $l[\sigma]$ .

As we will see if  $l[\sigma] < 0$  there are only three regions in the phase diagram namely the high-density, the low-density and the maximum current phases. On the other hand if  $l[\sigma] \geq 0$ , the high density phase disappears and only the low-density and the maximum current phases remain. We call these two regimes, the 3-phase and 2-phase regimes respectively. Qualitatively the transition from the 3-phase to the 2-phase regime is accomplished by shifting the distribution function from low speeds to higher speeds. As an example if  $P(v_1) \neq 0$  (i.e: if there is a significant relative probability of injecting slow particles to the system), then it is clear that  $\lim_{v \rightarrow v_1^-} g(v) = \infty$  and hence  $l[\sigma] = 0$ , which means that we are in the 3-phase regime. The case of discrete values of particle velocities is a special case in this category. However if  $\sigma(v)$  approaches zero slowly enough as  $v$  approaches  $v_1$ , (i.e: if the chance of entrance of slow cars is small), then we will be in the two phase regime. The exact criteria is given by the parameter  $l[P_c] = 0$ .

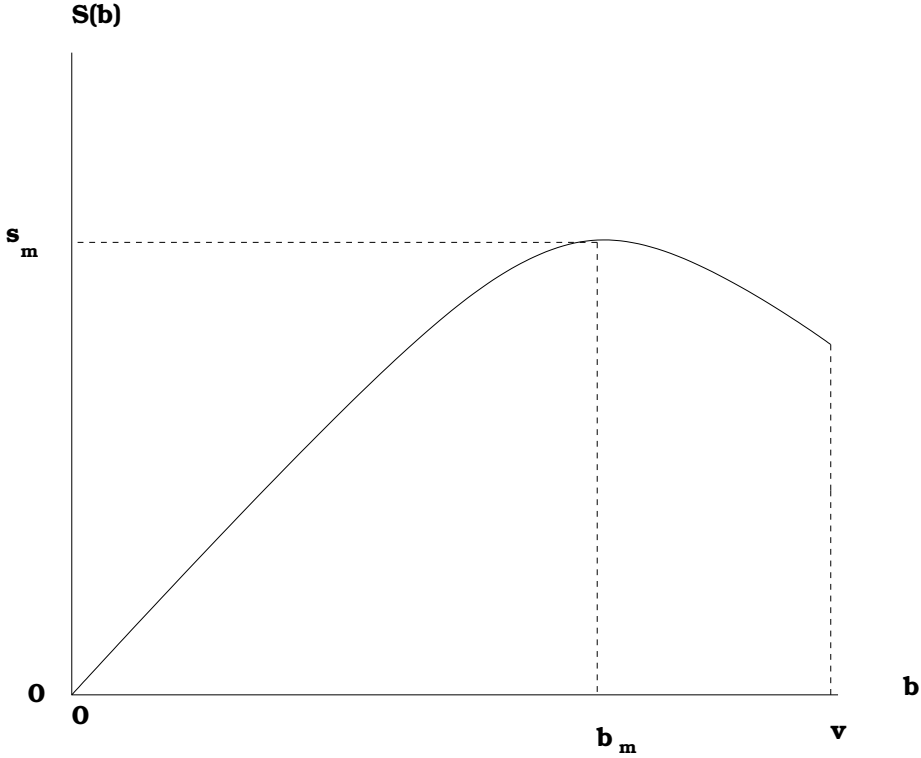


Figure 5: The generic form of the function  $S(b)$  (here  $l[\sigma] < 0$ )

#### 4.1 The singularities of the generating function $f(s; a, b)$

In order to determine the phases we have to determine the singularities of the generating function. For the

case  $l[\sigma] < 0$  where  $S$  has a maximum  $s_m$  at  $b_m \in (0, v_1)$  (Fig. 5), we define two right inverses for  $S$ .

One is the function  $B$  defined in the previous section. It is defined in the interval  $[0, s_m]$ , and has the following properties.

$$\begin{cases} S[B(s)] = s, & 0 \leq s \leq s_m \\ B[S(b)] = b, & 0 \leq b \leq b_m \end{cases} . \quad (49)$$

The other function is  $\tilde{B}$ , defined in  $[S(v_1), s_m]$ , with the following properties

$$\begin{cases} S[\tilde{B}(s)] = s, & S(v_1) \leq s \leq s_m \\ \tilde{B}[S(b)] = b, & b_m \leq b \leq v_1 \end{cases} . \quad (50)$$

The graphs of these functions are shown in figure 6.

We now consider the generating function as given in (39). The singularities of  $f$  as a function of  $s$  may

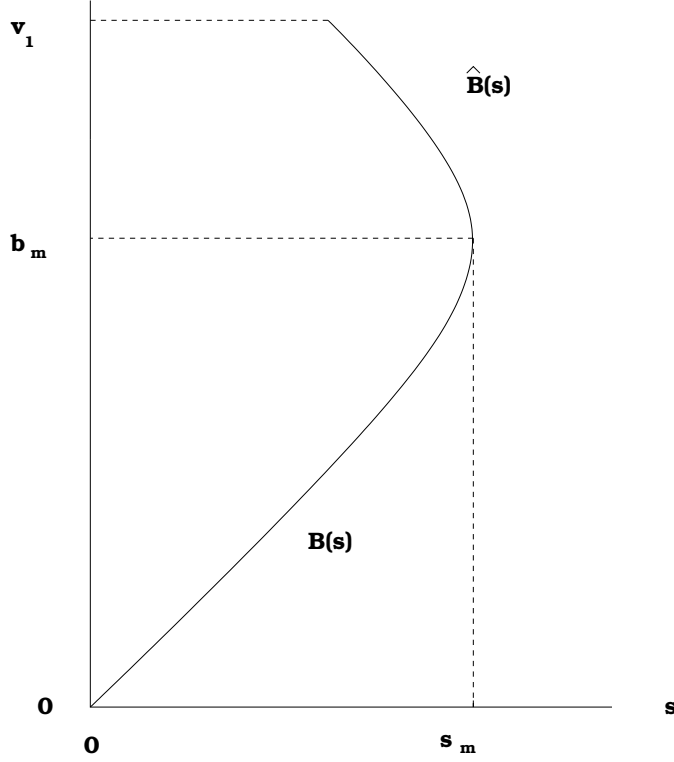


Figure 6: The functions  $B(s)$  and  $\tilde{B}(s)$

be of one of following types. The first singularity denoted be  $s_\alpha$  may arise from vanishing of  $(1 - aB(s))$  in the numerator. That is

$$B(s_\alpha) = \frac{1}{a} = \alpha, \quad (51)$$

or

$$s_\alpha = S(\alpha). \quad (52)$$

However (51) has a real positive solution for  $s$  if and only if  $\alpha = (1/a) < b_m$  (see fig.(6)). Thus  $s_\alpha$  is a singularity provided that  $\alpha < b_m$ .

The second singularity which we denote by  $s_\beta$  may arise from vanishing of the denominator, i.e:

$$s_\beta = S(b) = S(1 - \beta). \quad (53)$$

However for  $b < b_m$ , according to (49) the numerator vanishes as well, and  $s_\beta$  is no longer a singularity,

which means that  $s_\beta$  is a singularity only when  $b > b_m$  (or  $\beta < 1 - b_m$ ).

Finally,  $B$  itself becomes singular at  $s = s_m$ . Notice that  $s_m$  is greater than  $s_\alpha$  and  $s_\beta$  both, provided these latter two exist (see fig.(5)).

In the next subsection we use these informations to determine the phases.

## 4.2 The phase structure for $l < 0$

In this case, the generating function has three singular points, namely  $s_\alpha$ ,  $s_\beta$  and  $s_m$ , each phase (the analytic expression of the current) is determined according to which of these singular points are the smallest.

- **The low density phase ( $s_\alpha < s_\beta, s_m$ ):**

In this phase which develops when  $\alpha < b_m$  and  $S(\alpha) < S(1 - \beta)$ , we have:

$$J = S(\alpha), \quad (54)$$

- **The high density phase ( $s_\beta < s_\alpha, s_m$ ):**

In this phase which develops when  $\beta < 1 - b_m$  and  $S(1 - \beta) > S(\alpha)$ , the total current is given by

$$J = S(1 - \beta), \quad (55)$$

and finally

- **The maximum current phase ( $s_m$  is the only singularity):** This phase exists for the rectangular area  $\alpha > b_m$  and  $\beta > 1 - b_m$ . The current is given by

$$J = s_m. \quad (56)$$

Summarizing we have:

$$J = \begin{cases} S(\alpha), & \alpha < b_m, \text{ and } S(\alpha) < S(1 - \beta) \\ S(\beta), & \beta < 1 - b_m, \text{ and } S(1 - \beta) < S(\alpha) \\ s_m = S(b_m), & \alpha > b_m, \text{ and } \beta > 1 - b_m \end{cases} \quad (57)$$

The phase diagram is shown in fig.(2). The coexistence curve between the low and high density phases is obtained by the nontrivial solution of the equation  $S(\alpha) = S(1 - \beta)$ . A parametric representation of this curve is:

$$\begin{cases} \alpha = B(s) \\ \beta = 1 - \tilde{B}(s) \\ S(v_1) < s < s_m \end{cases} \quad (58)$$

We see that the main features of the 1-ASEP diagram are present. In this regime the multi-species nature of the process has only a minor effect. We will see that this exact result is also substantiated by a domain wall analysis in accordance with the analysis of [30].

### 4.3 The phase structure for $l \geq 0$

In this case the generating function has only two singular points, namely  $s_\alpha$  and  $s_m = S(v_1)$ . Consequently we have only two phases (Fig. (4)).

- The low density phase in which

$$J = S(\alpha), \quad (59)$$

and

- The maximum current phase in which

$$J = S(v_1). \quad (60)$$

In summary

$$J = \begin{cases} S(\alpha), & \alpha \leq v_1 \\ S(v_1), & \alpha > v_1 \end{cases} \quad (61)$$

The high-density phase has been shrunk and lost, and the injection parameter determines which phase we have. This is due to the fact that in this regime the current density diagram is monotonically increasing (see section 7) and hence according to the domain wall analysis, only the low density and the maximum current phases are expected to exist. Moreover in the maximum current phase everything is controlled by the lowest-speed particles.

The disappearance of the maximum density phase has an interesting implication, for the occurrence of traffic jams and its dependence on the bulk parameters beside the boundary ones. From the above analysis one can conclude that the maximum density or traffic jam occurs only when there is a critical probability of having particles or cars of slow velocities, the exact criteria is given by the parameter  $l$  defined above.

## 5 Exact calculation of the generating function $f(\mathbf{z}; s; a, b)$ and the average densities of each species

Using the same calculation which led to (36), we obtain

$$\frac{1}{s}[f(\mathbf{z}; s; a, b) - f(0; a, b)] = \oint \frac{du}{2\pi i u} f(\mathbf{z}; s; a, u) \left[ g(\mathbf{z}; b) + \frac{z_0}{u} \right] \frac{1}{1 - b/u}, \quad (62)$$

and from that we arrive at an expression analogous to (38)

$$f(\mathbf{z}; s; a, b) = \frac{z_0 s f(\mathbf{z}; s; a, 0) - b f(\mathbf{z}; 0; a, b)}{b \{s[g(\mathbf{z}; b) + z_0/b] - 1\}} \quad (63)$$

where

$$g(\mathbf{z}; b) := \left\langle \frac{z}{1 - b/v} \right\rangle = \int dv \sigma(v) \frac{z(v)}{1 - b/v}. \quad (64)$$

Note that for a continuous distribution  $\sigma(v)$ , the parameters  $z_i$  are replaced by a function  $z(v)$ . From (63), by a reasoning exactly the same as that of section 2, we arrive at

$$f(\mathbf{z}; s; a, b) = \frac{\frac{B(\mathbf{z}; s)}{1 - a B(\mathbf{z}; s)} - \frac{b}{1 - a b}}{b \left[ \frac{s}{S(\mathbf{z}; b)} - 1 \right]}, \quad (65)$$

where

$$\frac{1}{S(\mathbf{z}; b)} := \frac{z_0}{b} + g(\mathbf{z}; b), \quad (66)$$

and  $B(\mathbf{z}; s)$  is that right-inverse of  $S(\mathbf{z}; b)$  which tends to zero as  $s \rightarrow 0$ .

According to (34), or its analogue for the case of continuous distribution, the average density of particles of speeds between  $v$  and  $v + dv$ .

$$\rho(v) = z(v) \frac{\delta}{\delta z(v)} \ln \frac{1}{R(\mathbf{z})} \Big|_{\mathbf{z}=\mathbf{1}}. \quad (67)$$

Knowing the smallest singularity of  $f(\mathbf{z}; s; a, b)$  is sufficient to obtain the average densities  $\rho(v)$ . Once again, we can distinguish three phases: the low-density phase, the high-density phase, and the maximum-current phase. In the low density phase  $R(\mathbf{z}) = S(\mathbf{z}, \alpha)$ . Thus  $\rho(v)$  is obtained from (64,66) and (67) as follows:

$$\rho(v) = z(v) \frac{\delta}{\delta z(v)} \ln \left[ \frac{z_0}{\alpha} + \int dv \sigma(v) \frac{z(v)}{1 - \alpha/v} \right] \Big|_{\mathbf{z}=\mathbf{1}} = \frac{\sigma(v) S(\alpha)}{1 - \frac{\alpha}{v}}. \quad (68)$$

The expression for the high-density phase is similar and reads

$$\rho(v) = \frac{\sigma(v) S(1 - \beta)}{1 - (1 - \beta)/v}. \quad (69)$$

The treatment of the maximum current phase however requires more care. If the the two phase regime (i.e:  $l \geq 0$ ), where the function  $S$  does not attain any maximum in  $[0, v_1]$ , the maximum current is  $S(v_1)$ , the situation is the same as above, and we have

$$\rho(v) = \frac{\sigma(v) S(v_1)}{1 - v_1/v}. \quad (70)$$

In the 3-phase regime (i.e:  $l < 0$ ) however, the maximum current is  $S(b_m)$ , where  $b_m$  itself depends on  $\mathbf{z}$ .

Therefore,

$$\frac{\delta}{\delta z(v)} \frac{1}{S[\mathbf{z}, b_m(\mathbf{z})]} \Big|_{\mathbf{z}=\mathbf{1}} = \frac{\delta}{\delta z(v)} \frac{1}{S(\mathbf{z}, b_m)} \Big|_{\mathbf{z}=\mathbf{1}} + \frac{\delta b_m(\mathbf{z})}{\delta z(v)} \Big|_{\mathbf{z}=\mathbf{1}} \frac{\partial}{\partial b} \frac{1}{S(b)} \Big|_{b=b_m}. \quad (71)$$

The second term in the right-hand side is, however, zero, since  $\frac{1}{S}$  is minimum at  $b_m$ . So we arrive at the expression

$$\rho(v) = \frac{\sigma(v)S(b_m)}{1 - b_m/v}. \quad (72)$$

To summarize, we have

$$\rho(v) = \frac{\sigma(v)S(x)}{1 - x/v}, \quad (73)$$

where

$$x = \begin{cases} \alpha, & \text{low-density phase} \\ 1 - \beta, & \text{high-density phase} \\ b_m, & \text{maximum current phase in the three-phase system} \\ v_1, & \text{maximum current phase in the two-phase system} \end{cases}. \quad (74)$$

The average density of vacant sites  $\rho_0$  can also be obtained either by using the formula  $\rho_0 = z_0 \frac{\partial}{\partial z_i} \ln \frac{1}{R(\mathbf{z})} \Big|_{\mathbf{z}=\mathbf{1}}$

or by using the sum rule

$$\rho_0 + \int dv \rho(v) = 1. \quad (75)$$

From (75), one obtains for each phase determined by the parameter  $x$  defined in (74)

$$\rho_0 = 1 - \int dv \frac{\sigma(v)S(x)}{1 - x/v}. = 1 - S(x)g(x) \quad (76)$$

where  $S(x) = S(\mathbf{1}, x)$  and  $g(x) = g(\mathbf{1}, x)$ . After using (66), this gives

$$\rho_0 = 1 - S(x) \left( \frac{1}{S(x)} - \frac{1}{x} \right) = \frac{S(x)}{x}. \quad (77)$$

## 6 Examples

### 1-The single species ASEP:

All we need to know to treat this special case is the function  $S(b)$  as given in eq.(47). Since there is only one kind of particle with  $v = 1$  we have

$$g(b) = \frac{1}{b(1-b)} \quad (78)$$

with  $l = 0$ ,  $b_m = \frac{1}{2}$ , and  $s_m = \frac{1}{4}$ . Thus according to (57) we have the following phases:

$$J = \begin{cases} \alpha(1-\alpha) & \alpha < \beta, \quad \text{and} \quad \alpha < \frac{1}{2} \\ \beta(1-\beta) & \alpha > \frac{1}{2}, \quad \text{and} \quad \beta < \frac{1}{2} \\ \frac{1}{4} & \alpha \geq \frac{1}{2}, \quad \text{and} \quad \beta \geq \frac{1}{2} \end{cases} \quad (79)$$

### 6.1 A hopping rate much lower than the others:

The case of a fixed or moving impurity has been studied in many previous works as for example in [27, 28, 29].

In the present framework we can consider a new case where the number of impurities is not one or even fixed. That is we allow very slow particles to have a chance of entering into and leaving the system.

Let one of the particles have a speed much lower than the rest: that is :  $b < v_1 <<< v_2 < v_3 < \dots < v_p$ .

Then with the approximation  $1 - \frac{b}{v_i} \approx 1$ , for  $i = 2, 3, \dots, p$ , one can write:

$$g(b) \equiv \frac{1}{p} \sum_{i=1}^p \frac{1}{1 - \frac{b}{v_i}} \approx \frac{1}{p} \left( \frac{1}{1 - \frac{b}{v_1}} + p - 1 \right) \quad (80)$$

from whcih one obtains:

$$S^{-1}(b) \equiv \frac{1}{b} + g(b) = \frac{b+1}{b} + \frac{b}{p(v_1 - b)} \quad (81)$$

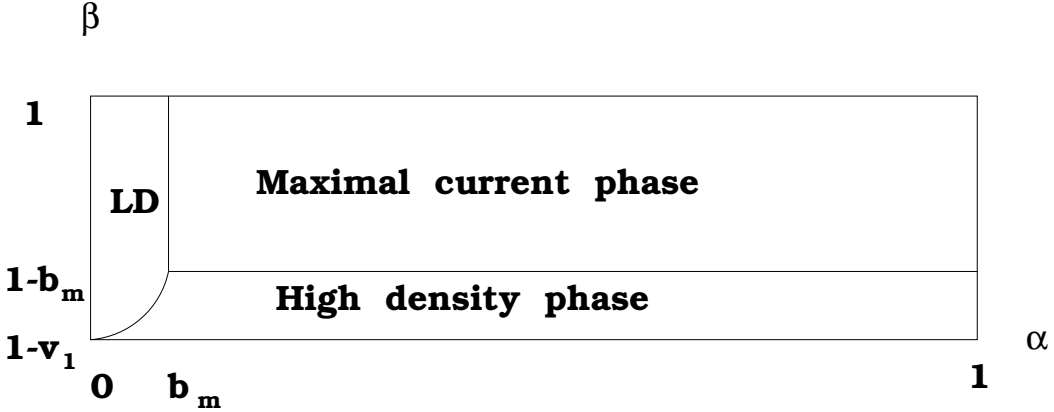


Figure 7: Phase diagram of the multi-species ASEP when one of the hopping rates is much smaller than the others.

For this function we have:

$$b_m = \frac{v_1}{1 + \sqrt{\frac{v_1}{p}}} \quad \text{and} \quad s_m = \frac{v_1}{1 + v_1 + 2\sqrt{\frac{v_1}{p}}} \quad (82)$$

Besides  $v_1, \alpha$  and  $\beta$ , only the number of species plays a role here.

The phase diagram is shown in Fig.(7).

The following features are readily observed. Compared to the other two phases, the size of the low density region is very small, as we expect on physical ground. Only for very small injection rate  $\alpha$  and for very large extraction rate  $\beta$  this phase can exist in the system. Even in the maximal current phase the current which is given by  $s_m$  is seen to be small and limited by the speed of the lowest particles. For fixed  $\alpha, \beta$ , and  $v_1$ , as the number of species  $p$  increases, the value of  $b_m$  approaches  $v_1$  and hence the high density phase begins to shrink, leaving only two phases in the system.

It is instructive to calculate the relative numbers of particles of different types including holes in each of the above phases. From (73) we find

$$\frac{\rho(v_i)}{\rho(v_1)} = \frac{1 - \frac{x}{v_1}}{1 - \frac{x}{v_i}} \quad (83)$$

where in each phase  $x$  is given as in (74). Inserting the relevant values of  $x$  and in the approximation

$\frac{b}{v_i} \ll 1 \quad \forall i \geq 2$ , we find:

$$\frac{\rho(v_i)}{\rho(v_1)} = \begin{cases} \frac{1 - \frac{\alpha}{v_1}}{1 - \frac{\alpha}{v_i}}, & \text{Low-density phase} \\ 1 - \frac{b}{v_1}, & \text{High-density phase} \\ 1 - \frac{b_m}{v_1}, & \text{maximal current phase} \end{cases} \quad (84)$$

In the low density region where  $\alpha$  takes values from 0 to  $b_m$ , this ratio takes values from 1 to  $1 - \frac{b_m}{v_1} = 1 - \frac{1}{1 + \sqrt{\frac{v_1}{p}}}$ . Thus in this region almost all types of particles are present in the system. In the high density region this ratio is at most equal to  $1 - \frac{1}{1 + \sqrt{\frac{v_1}{p}}}$  which is determined by the interplay of the lowest speed and the number of species. For large  $p$ , it is indeed a very small value, indicating that the system is almost filled by the lowest particles

This ratio takes its maximum value in the entire maximal current phase. One can also obtain the ratio of the density of lowest speed particles to that of the holes. From (73) and (77) one obtains

$$\frac{\rho(v_1)}{\rho_0} = \begin{cases} \frac{1}{p} \frac{\alpha}{1 - \frac{\alpha}{v_1}}, \\ \frac{1}{p} \frac{b}{1 - \frac{b}{v_1}} \\ \frac{1}{p} \frac{b_m}{1 - \frac{b_m}{v_1}} \end{cases} \quad (85)$$

where from top to bottom we have listed the low density, the high density and the maximal current phases. Again we can find the limiting values of this ratio, to see how crowded the system is, in each phase. It is simple to see that the ratio ranges from 0 to  $\sqrt{\frac{v_1}{p}}$  in the low density, and from  $\sqrt{\frac{v_1}{p}}$  to infinity, in the high density and is fixed at  $\sqrt{\frac{v_1}{p}}$  in the maximal current phase.

With a little more effort, starting from (81), the coexistense line between the low-density and the high-density phases is found to be given by:

$$\beta = \alpha + 1 - \frac{pv_1^2 + \alpha^2(v_1 - p)}{(\alpha + p)v_1 - \alpha p} \quad (86)$$

## 7 Discussion

The results that we have obtained on the phases and currents are exact. We can get a feeling for these results, based on the intuitive arguments of domain wall dynamics [4, 31, 27, 14, 30]. What we will do in this section is to formally adopt the analysis of [30] and rederive our exact results. The essential result of [30] is that for all single species processes which have single peak current density relation, the phase diagram of the ASEP is generic, that is the possible phases are the low density, the high density and the maximal current phases. Roughly speaking one expects that for  $\alpha$  small and  $\beta$  large, the low density phase denoted schematically by (000000000), prevails in the system, and for  $\alpha$  large and  $\beta$  small, the high density phase denoted by (11111111) prevails. However when there is no restriction on the injection and extraction rates of the particles, that is for  $\alpha$  and  $\beta$  large, the current reaches its maximum value allowed in the current density diagram, this new phase being called the maximal current phase and denoted by (mmmmmmmm). The exact shape of the phase diagram and the coexistence lines are obtained by studying the dynamics of a supposedly formed domain wall at sufficiently late times between any pair of these phases under appropriate conditions. For example when  $\alpha$  is small and  $\beta$  is large, the late time configuration is supposed to be (000000111111). It is also assumed that deep into each of the two segments we have a product measure with constant density. This assumption is well founded [4, 31, 27, 14] by numerical, mean field and exact solutions. The velocity of such a domain wall is then given by the formula

$$V = \frac{J_o - J_1}{\rho_0 - \rho_1}, \quad (87)$$

where  $J_0$  and  $\rho_0$  ( resp.  $J_1$  and  $\rho_1$  ) are the current and density to the far left ( resp. right ) of the domain wall. The sign of this velocity determines the prevailing phase and setting this velocity equal to zero determines the coexistence line. In the latter case the two phases coexist due to dominance of fluctuations

in the rms position of the domain wall. For the currents and the densities in (87) one uses the mean field values. For the maximal phase, one uses the density which maximizes the current in the current density diagram.

The above analysis can be readily applied to the multi-species case. On the assumption that the coarse grained bulk current is given by the uncorrelated Bernoulli measure [32], we can use the one-parameter family of one dimensional representations for the bulk relations in (6-7) to obtain [20]

$$E = \frac{1}{b} \quad D_i = \frac{v_i}{v_i - b} \quad (88)$$

and consequently the following forms for current and total density:

$$J(b) = \left( E + \frac{1}{p} \sum_{i=1}^p D_i \right)^{-1} = \left( \frac{1}{b} + \left\langle \frac{v}{v-b} \right\rangle \right)^{-1} \quad (89)$$

$$\rho(b) = \left\langle \frac{v}{v-b} \right\rangle \left( \frac{1}{b} + \left\langle \frac{v}{v-b} \right\rangle \right)^{-1} \quad (90)$$

Note that the right hand side of (89) is exactly the function  $S(b)$  defined in equation (40). However, before using equation (87), we need to determine the free parameter  $b$  and its range, in the Bernoulli measure for each phase. For the maximum current phase the parameter is obviously  $b_m$  which maximizes  $J(b)$ . This is exactly the parameter which has been defined in section (4.1). For the other two boundary-controlled phases, the parameter  $b$  should be fixed by compatibility with the boundary conditions of (8-9), according to which a product measure coupled to a left reservoir injecting particles at rate  $\alpha$  should have  $b = \alpha$  and a product measure coupled to a right reservoir extracting particles at rate  $\beta$  should have  $b = 1 - \beta$ . Instead of using this type of argument which is based on MPA relations one can follow the more general argument suggested in [14], to match the boundary rates with the bulk densities.

Note also that for the low density phase  $b < b_m$  and for the high density phase  $b > b_m$ . Thus we have

$J_0 = J(b = \alpha)$ ,  $J_1 = J(b = 1 - \beta)$  and  $J_m = J(b_m)$ . Equating the currents we obtain exactly the phase

structure previously obtained by exact solution. Moreover the size of the maximum density region in the phase diagram depends on the value  $v_1 - b_m$  (see Fig. (5)). When  $v_1 - b_m$  approaches zero, the size of this region shrinks and we remain only with two phases. This is again in accord with our exact solution.

To conform completely to the picture advocated in [30] we should have discussed various phases according to the behaviour of the function  $J(\rho)$  and not the function  $J(b)$ . However in our case the qualitative behaviour of these two functions resemble each other. In fact it is seen from (89-90) that  $\rho$  is a monotonically increasing function of  $b$ , which attains its maximum  $\rho_1$  at  $b = v_1$ . Moreover  $J(\rho = 0) = 0$ ,  $J'(\rho = 0) = 1$ , and finally [21]  $J$  is a convex function of  $\rho$ . To see if  $J(\rho)$  attains a local maximum in its domain of definition  $[0, \rho_1]$  or not we evaluate  $\frac{dJ}{d\rho}$  at  $\rho = \rho_1$  and find

$$\frac{dJ}{d\rho}(\rho_1) = \frac{\frac{dJ}{db}(v_1)}{\frac{d\rho}{db}(v_1)} = \frac{\frac{1}{v_1^2} - \left\langle \frac{v}{v-v_1} \right\rangle}{\frac{1}{v_1^2} \left\langle \frac{v}{v-v_1} \right\rangle}, \quad (91)$$

Thus here also the value of the parameter  $l$  determines the answer to the above question.

We should stress that the above arguments due to their qualitative nature are not by no means a substitute for exact solutions. However it is remarkable that in view of the crude approximations involved, they can predict exact results.

## 8 Acknowledgement

The authors wish to thank the hospitality provided by the Abdus Salam International Center for Theoretical Physics where this work was completed.

## References

1. B. Schmittmann and R. K. P. Zia in "Phase transitions and critical phenomena" vol. 17, eds. C. Domb and J. Lebowitz (London, Academic Press, 1995).
2. F. Spitzer, Adv. Math. **5**,246(1970).
3. T. M. Liggett, *Interacting Particle Systems* (Springer-Verlag, New York, 1985).
4. H. Spohn, *Large Scale Dynamics of Interacting Particles* (Springer-Verlag, New York, 1991).
5. D. Dhar, Phase Transitions **9**,51 (1987).
6. B. Derrida, Phys. Rep. **301**, 65 (1998).
7. J. Krug and H. Spohn in *Solids Far From Equilibrium*, C. Godreche, ed. (Cambridge University Press,1991).
8. D. Helbing and B. A. Huberman, Nature; 396,738 (1998).
9. D. Helbing and M. Schreckenberg, Phys. Rev. E **59**, R2505(1999).
10. M. R. Evans, N. Rajewsky and E. R. Speer; Exact solution of a cellular automaton of traffic, cond-mat/9810306.
11. B. Derrida and M. R. Evans in "Non-Equilibrium Statistical Mechanics in one Dimension", V. Privman ed. (Cambridge University Press, 1997).
12. G. M. Schütz; Integrable stochastic processes in *Phase Transitions and Critical Phenomena*; eds. C. Domb and J. Lebowitz (Academic Press, New York, 1999).
13. G. Schütz; Phys. Rev. E **47**,4265(1993), J. Stat. Phys. **71**,471(1993).

14. G. Schütz and E. Domany; *J. Stat. Phys.* **72** 277(1993).
15. B. Derrida, M.R. Evans, V. Hakim and V. Pasquier, *J.Phys.A:Math.Gen.* **26** 1493(1993).
16. B. Derrida, E. Domany and D. Mukammel; *J. Stat. Phys.* **69** 667(1992).
17. K. Krebs and S. Sandow; *J.Phys. A ; Math. Gen.* **30** 3165(1997).
18. P. Arndt, T. Heinzel and V. Rittenberg; *J.Phys. A ; Math. Gen.* **31** 833(1998).
19. F. C. Alcaraz, S. Dasmahapatra and V. Rittenberg V *J.Phys. A ; Math. Gen.* **31** 845 (1998).
20. V. Karimipour, *Phys. Rev. E* **59** 205 (1999).
21. V. Karimipour, "A multi-species asymmetric exclusion process, steady state and correlation functions on a periodic lattice" *cond-mat/9809193*, to appear in *Europhys. Lett.*(1999).
22. M. R. Evans; *J. Phys. A: Math. Gen.* **30** 5669(1997); *Europhys. Lett.* **36** 13 (1996).
23. M. R. Evans, D. P. Foster, C. Godreche D. Mukamel; *J. Stat. Phys.* **80** (1995); *Phys. Rev. Lett.* **74**,208(1995).
24. H. W. Lee, V. Popkov, and D. Kim ; *J.Phys. A ; Math. Gen.* **30** 8497 (1997).
25. K. Mallick, S. Mallick, and N. Rajewsky; Exact Solution of an exclusion process with three classes of particles and vacancies; *cond-mat/9903248*.
26. M. E. Fuladvand and F. Jafarpour; Multi-species asymmetric exclusion process in ordered sequential updates, *cond-mat/9901007*, to appear in *J. Phys. A; Math. Gen.*
27. S. A. Janowsky and J. L. Lebowitz; *Phys. Rev. A* **45**,618 (1992).

28. B. Derrida, S. A. Janowsky, J. L. Lebowitz and E. R. Speer; *J. Stat. Phys.* **78**, 813(1993); *Europhys. Lett.* **22**, 651(1993).
29. K. Mallick; *J. Phys. A* **29**, 5375(1996).
30. A. B. Kolomeisky et al.; *J. Phys. A; Math. Gen.* **31**(1998)6911.
31. E. D. Andjel, M. Bramson, and T. M. Liggett; *Prob. Theor. Relat. Fields*, **78**, 231 (1998).
32. J. L. Lebowtiz, E. Presutti, and H. Spohn; *J. Stat. Phys.* **51** , 841(1988).

## Figure Captions

Fig. 1: The phase diagram for the single species ASEP.

Fig. 2: The phase diagram for the p-species ASEP for a typical distribution of hopping rates when  $l[\sigma] < 0$ .

Fig. 3: Two phase diagrams for the p-species ASEP for different distributions of hopping rates. In both cases  $l[\sigma] < 0$ .

Fig. 4: The phase diagram for the p-species ASEP when  $l[\sigma] > 0$ .

Fig. 5: The generic form of the function  $S(b)$  which produces the three phase regime.

Fig. 6: The inverse functions of  $S(b)$ .

Fig. 7: The phase diagram for the case when one of the hopping rates is much smaller than the others.